

Inelastic scattering of electrons by adsorbate vibrations in the impact scattering regime: CO on Ni(100) as an example

S. Y. Tong and C. H. Li

Department of Physics, The University of Wisconsin-Milwaukee, Milwaukee, Wisconsin 53201

D. L. Mills

Department of Physics, University of California, Irvine, California 92717

(Received 12 December 1980)

We have used a formalism developed by us recently to carry out a series of calculations of electron-energy-loss (EELS) cross sections for excitations of vibrations in a $c(2\times 2)$ overlayer of CO on the Ni(100) surface. The calculations explore impact scattering and cover a wide range of energies and scattering geometries. We examine the sensitivity of the various cross sections to the CO bond length, and also to the C-Ni distance. We also find a series of selection rules that apply to the impact-scattering problem. These are discussed and illustrated with numerical calculations of the angular variation of the EELS cross sections.

I. INTRODUCTORY REMARKS

Electron-energy-loss spectroscopy (EELS) has become a most important experimental method in the study of molecules adsorbed on single crystal surfaces,¹ and we are just beginning to see the method extended to the study of the vibrational motion of atoms in single crystal surfaces.² In the experiment, a highly monoenergetic electron beam is directed toward the surface of interest, and one analyzes the energy spectrum of electrons scattered inelastically by the vibrational motion of atoms or molecules on the crystal surface. The method is, for surface physics, a direct analog of the neutron scattering experiments that have played a crucial role in the elucidation of the dynamical properties of a wide range of solid materials.

In the best spectrometers available at this date, one may achieve an energy resolution of only 30 cm^{-1} (3.7 meV), so when EELS is compared to optical spectroscopy, the method offers poor resolution. However, in the experiment, one is probing the surface with particles with a de Broglie wavelength comparable to crystal lattice constants or molecular bond lengths, so the EELS method can in principle be used to probe microscopic structural details of the surface geometry. In contrast to this, optical spectroscopies all employ long wavelength probes and are sensitive only to overall symmetry as a consequence. This paper presents detailed theoretical calculations which explore the sensitivity of the EELS cross sections to microscopic details of the adsorption geometry, for a $c(2\times 2)$ layer of CO adsorbed on the Ni(100) surface. The calculations are based on a formalism developed recently by us.³ Some of the results have been presented briefly else-

where,⁴ and since this early discussion we have carried out an extensive series of new calculations. We present a discussion of our analysis of electron scattering from a monolayer of CO adsorbed on Ni(100) here, and it is our intention in a subsequent paper to report similar calculations for H adsorbed on W(100). A detailed comparison of the calculated EELS cross sections for these very different systems should prove most illuminating. Before we turn to a presentation of our results, a few introductory remarks may prove helpful.

All of the early experimental studies of inelastic scattering of low-energy electrons by adsorbate vibrations and many studies currently underway, examine only those inelastically scattered electrons which emerge very close to the specular direction. The acceptance angle is typically one or two degrees. When a molecule is placed on a metal surface, the vibrational modes which generate an oscillating electric dipole moment with component normal to the surface produce a strong electrostatic potential above the surface, and this potential scatters the electron strongly. Electrons scattered by this mechanism emerge very close to the specular direction; a typical deflection angle $\Delta\theta$ from the specular is $\Delta\theta \cong \hbar\omega_0/2E_0$, where ω_0 is the frequency of the vibration and E_0 is the impact energy. One has $\Delta\theta \cong 0.1^\circ$ in a typical experiment. A proper quantum-mechanical theory of the dipole scattering mechanism⁵ shows the EELS cross section is a product of a function $f(E_0, \Delta\theta)$ that describes the dipole excitation probability and, when certain conditions are met,⁶ the intensity I_0 of the specular beam. As the electron impact energy E_0 is decreased, $f(E_0, \Delta\theta)$ increases until the characteristic angle $\Delta\theta$ exceeds the spectrometer slit width. At the same time, I_0 increases with de-

creasing energy, so for dipole scattering the maximum signal is obtained when low impact energies in the range of 1 to 5 eV are employed. To first approximation, vibrational modes with electric dipole moment parallel to the surface fail to scatter near the specular, since their dipole moment is nearly cancelled by the image dipole in the substrate.⁵ Thus, we have the dipole selection rule mentioned earlier.

Far from the specular, even for a mode polarized normal to the surface, the simple dipole theory breaks down and a proper description of the EELS cross section requires a microscopic theory which takes due account of the detailed structure of the potential of adsorbate molecule and underlying substrate. One may see this as follows. In the dipole scattering theory, if the electron wavevector transfer has magnitude Q_{\parallel} , the electron scatters from electric field fluctuations in the vacuum above the crystal when it is a distance $l_0 \cong Q_{\parallel}^{-1}$ from the surface. For a 5-eV electron deflected 20° off specular, one has $l_0 \cong 2.5 \text{ \AA}$. When l_0 is so small, a microscopic theory is required that takes detailed account of the structure of the crystal potential and electron penetration into the substrate, and the long-range dipole tail of the scattering potential becomes unimportant. The same remark applies to inelastic scattering produced near the specular direction by "dipole-forbidden" modes, or possibly those characterized by small values of the dipole-moment effective charge (this is frequently called the polarizability derivative in the chemical literature).

It is useful to introduce terminology which draws a distinction between situations where the dipole mechanism and the associated long-ranged electrostatic fields dominate the observed cross section, and where short-ranged interactions dominate. The latter regime is often called the impact-scattering regime since, in some crude sense, one may think of the scattering event as a collision between the electron and a collection of vibrating billiard balls. Quite clearly, it is impossible to draw a rigorous distinction between the two regimes since, for a dipole-active mode the near specular losses are controlled by long-ranged fields but as one moves off specular to very large angles where an impact-scattering picture is appropriate, the transition from the first regime to the second is smooth and continuous. As we shall see shortly in these introductory remarks, it is at present difficult to construct a single theory which includes a proper description of dipole scattering along with the microscopic details of the crystal potential. Thus, to the theorist it is useful to examine each regime separately. Fortunately, in the data the near specular "dipole lobe" is fre-

quently a striking feature that stands out distinctly above a broad angular distribution of inelastically scattered electrons.

Our recent theoretical effort^{3,4} and the detailed calculations reported here, are based on an impact-scattering description of the EELS process which takes full account of multiple scattering of the incoming and scattered electrons from the molecules in the adsorbed layer and within the substrate. As remarked earlier, we have developed a formalism³ that enables such calculations to be carried out through use of the multiple-scattering theories that have proven useful elsewhere in surface physics.

We have found⁴ that in the theory of impact scattering, there exist useful selection rules which supplement the well known dipole selection rule introduced by Evans and Mills.⁵ Our earlier discussion of the selection rules which operate for modes that scatter predominantly by impact scattering was brief,⁴ and here we discuss these in more detail and illustrate them with our numerical calculations. In the near future, it is likely that the selection rules will prove most useful to experimentalists equipped with present day spectrometers. To extract detailed structural information from the energy variation of the EELS cross section, it would be useful to construct spectrometers which operate at impact energies of a few tens of electron volts, rather than a few electron volts. This will be clear from the discussion below.

A new ingredient required in the theory is a description of the electron-phonon interaction. We have modeled this as follows. We begin with an array of muffin-tin potentials arranged to describe an (ordered) adsorbate layer and the underlying substrate. We form the matrix element for the electron-phonon interaction by rigidly displacing the muffin-tin potential associated with a site of interest and sandwiching the change in potential δV between the relevant wave functions that describe the incident and scattered electron. The details of this procedure have been given elsewhere,³ but for the present purposes one should note that this procedure never generates an electric dipole moment since the electron charge cloud, assumed spherically symmetric around each nucleus, follows the nucleus without distortion. Thus, within this formalism we describe impact scattering at large angles, but we are unable at the same time to recover the dipole contribution near the specular for dipole-allowed modes. Such calculations have proved exceedingly difficult in the highly developed field of electron-molecule scattering. An EELS theory with both impact and dipole scattering incorporated fully and

rigorously thus represents a major extension of the present study.

We believe one could synthesize useful formulas for the EELS cross sections by simply adding to our impact-scattering t matrix the additional dipole portion which is large near the specular for allowed modes. We have chosen not to use such a phenomenological procedure here, because we wish to focus our attention on the detailed behavior of the impact-scattering cross sections for the $c(2 \times 2)$ layer of CO on Ni. Before we turn to our detailed results, we briefly summarize some principal conclusions.

As remarked earlier, the cross section for dipole scattering decreases with increasing electron energy, because the dipole excitation functions $f(E_0, \Delta\theta)$ decreases and because the specular reflectivity I_0 does also. When we calculate $(dP_i/d\Omega)d\Omega$, the probability an electron is scattered into solid angle $d\Omega$ after exciting the i th vibrational mode of the adsorbate by impact scattering, we find a very different behavior. In the impact-scattering regime, the excitation probability *increases* with energy. More precisely, $(dP_i/d\Omega)$ is not a monotonic function of energy, but rather consists of a series of diffraction peaks superimposed on a background which increases with energy. The point is that as one moves to higher impact energies, the cross section for vibrational excitation by the impact mechanism increases on the average, while the specular intensity I_0 falls off. This suggests that it will be advantageous to work at higher beam energies, in the regime of 30–200 eV, to study vibrational excitation by impact scattering. Also, as we show here, the diffraction peaks have position and shape influenced by the microscopic details of the adsorption site geometry, as in other electron surface spectroscopies. We thus have very rich information in this energy regime, and it would be of very great interest to see experiments carried out with incident electron energy in this range.

We may quantify the above remarks as follows. For an impact energy of 5 eV, the calculations reported below show $(dP_{\omega_i^{(+)}}/d\Omega) \cong 10^{-4}$ for impact scattering, where here and elsewhere in this paper we refer to the CO stretch mode as the $\omega_i^{(+)}$ mode. If these electrons are collected with a slit geometry that collects all electrons that lie within a cone with apex half angle $\Delta\alpha = 1^\circ$, then the solid angle $\Delta\Omega$ subtended by the spectrometer slit is $\Delta\Omega \cong 10^{-3}$ steradians. Hence, roughly one electron out of each 10^7 in the *incident* beam is scattered into the spectrometer slits by the impact mechanism. For a strong dipole-allowed mode such as the CO stretch, about one electron in 10^5 is scattered from the *incident* beam into the near specu-

lar dipole lobe; for this estimate, we assume one percent of the electrons in the incident beam are contained in the specular beam of electrons scattered elastically from the surface. Thus, at these low incident electron energies, our calculations show the cross section for *large-angle* impact scattering to be roughly two orders of magnitude smaller than the near specular dipole lobe when the comparison is made as outlined.

Now consider incident electron kinetic energies in the range of 50 eV rather than 5 eV. The dipole cross section will be at least an order of magnitude smaller here than at 5 eV, when the combined energy variation of the dipole excitation function $f(E, \Delta\theta)$ and the specular intensity I_0 are considered. At the same time, our calculations show $(dP_{\omega_i^{(+)}}/d\Omega)$ increases by roughly one order of magnitude. Hence, the same comparison shows the near specular dipole-scattering intensity has fallen off sufficiently, and the impact-scattering cross section has increased to the point where the two signals are comparable in intensity near the specular even for a strong dipole-allowed mode.

The above remarks, combined with the diffraction features produced by multiple scattering of the electron from the adsorbate-substrate combination, lead us to suggest that experiments should be performed at incident electron energies substantially higher than those used at present.

There is one final general point we wish to stress before we turn to the discussion of our detailed calculations. As remarked above, when certain conditions are met,⁶ the near specular dipole cross section may be expressed as the product of the dipole excitation function $f(E, \Delta\theta)$ derived explicitly elsewhere,⁵ and the elastic intensity I_0 of the specular beam. It thus proves useful to divide the measured dipole-loss cross section by I_0 to obtain $f(E, \Delta\theta)$. By this means, quantitative values of the magnitude of the dipole-moment effective charge e^* may be extracted from the data.⁷ In the impact-scattering regime, as we emphasized earlier,⁴ the EELS cross section has its own characteristic variation with energy, and this bears no simple relation to the energy variation of the specular intensity I_0 . Thus, to divide impact-scattering-dominated EELS data by I_0 obscures rather than clarifies the information contained in the data, in general. This point is amply illustrated by Fig. 2 of Ref. 4, and we shall not discuss this issue in any more detail here.

We now turn to a discussion of our calculations. Section II presents a discussion of our calculations of the energy variation of the EELS cross sections, and Sec. III explores the selection rules which operate in the impact-scattering regime.

II. THE ENERGY VARIATION AND STRUCTURAL SENSITIVITY OF EELS CROSS SECTIONS

Before we turn to a presentation of the results of our numerical calculations, we recall the general features of the method of calculation.³

We begin with an array of muffin-tin potentials centered at sites $\{\vec{R}(\hat{I})\}$. The outermost layer of potentials describe the $c(2 \times 2)$ arrangement of oxygen ions, the next layer is the layer of carbon ions, and we then have the Ni substrate. If $\vec{R}_0(\hat{I})$ is a vector to the equilibrium position of the nucleus at site \hat{I} , then $\vec{R}(\hat{I}) = \vec{R}_0(\hat{I}) + \vec{u}(\hat{I})$, i. e., we consider an array of muffin-tin potentials, with $\vec{u}(\hat{I})$ the displacement of the nucleus at site \hat{I} from its equilibrium position.

If an electron of wave vector $\vec{k}^{(I)}$ is incident on this array, then we can calculate $f(\vec{k}^{(F)}, \vec{k}^{(I)}; \{\vec{R}\})$ the scattering amplitude for scattering into the final state $\vec{k}^{(F)}$ (in the vacuum above the adsorbate-substrate combination). As indicated, the scattering amplitude depends parametrically on the positions of the various nuclei. Then if $\vec{u}(\hat{I})$ is small, we may expand the scattering amplitude in powers of $\vec{u}(\hat{I})$. To first order in the displacement, with $u_\alpha(\hat{I})$ the α th Cartesian component of $\vec{u}(\hat{I})$,

$$f(\vec{k}^{(F)}, \vec{k}^{(I)}; \{\vec{R}\}) = f(k^{(F)}, k^{(I)}; \{\vec{R}^0\}) + \sum_{\alpha} \sum_{\hat{I}} \left(\frac{\partial f}{\partial R_{\alpha}(\hat{I})} \right)_0 u_{\alpha}(\hat{I}) + \dots \quad (1)$$

The first term in Eq. (1) describes elastic scattering from the structure with all nuclei at their equilibrium position (the low-energy-electron-diffraction problem), while the second term describes vibrational loss by one phonon process. In Ref. 3, we have analyzed the derivative $[\partial f / \partial R_{\alpha}(\hat{I})]_0$ within the framework of multiple scattering theory, and the calculations presented here are based on these results.

Quite clearly, from Eq. (1) we see that we need to know the amplitudes of the motion of the various ions to calculate the cross section for scattering from a particular vibrational mode of the system. We are interested here exclusively in inelastic scattering of electrons from the vibrations in the adsorbed CO layer,⁸ so we have supposed that the Ni atoms remain at rest always, and only the carbon and oxygen nuclei participate in the vibrational motion. For scattering from the CO stretch mode, this is clearly an excellent approximation, though it is more questionable for some of the lower-frequency modes, such as the C-Ni stretching mode. For reasons discussed below, we believe the calculations are not very sensitive to this assumption. We shall see that for a considerable range of energy and im-

pact angles, the EELS cross sections are not very sensitive to the C-Ni spacing, so inclusion of the motion of the Ni atoms is unlikely to affect the results greatly.

As in our earlier paper, we refer to the outermost layer of nuclei (the oxygens) as layer *A*, and the second layer (the carbons) as layer *B*. Furthermore, we suppose each CO molecule vibrates independently of the others. If $\delta f(\vec{k}^{(F)}, \vec{k}^{(I)}; \{\vec{R}\})$ is the part of the scattering amplitude which is first order in $\vec{u}(\hat{I})$, and $\vec{Q}_{\alpha} = \vec{k}_{\parallel}^{(F)} - \vec{k}_{\parallel}^{(I)}$ is the wave-vector transfer of the electron projected onto a plane parallel to the surface, we have

$$\delta f(k^{(F)}, k^{(I)}; \{R\}) = \sum_{\alpha} \delta f_{A\alpha}^{(1)}(\vec{Q}_{\parallel}) u_{\alpha}^{(A)} + \sum_{\alpha} \delta f_{B\alpha}^{(1)}(\vec{Q}_{\parallel}) u_{\alpha}^{(B)}, \quad (2)$$

where

$$\delta f_{A\alpha}^{(1)}(\vec{Q}_{\parallel}) = \frac{1}{\sqrt{N_s}} \sum_{\hat{I}_{\parallel}} \left(\frac{\partial f}{\partial R_{A\alpha}(\hat{I}_{\parallel})} \right)_0 \exp[i\vec{Q}_{\parallel} \cdot \vec{R}_A^{(0)}(\hat{I}_{\parallel})], \quad (3)$$

and $\vec{u}^{(A)}$, $\vec{u}^{(B)}$ are suitably normalized eigenvectors of the vibrating adsorbate molecule.

For our $c(2 \times 2)$ layer of CO on the Ni(100) surface, with the CO standing vertically and terminally bonded, the normal modes are polarized either normal to the surface or parallel to the surface. For this site, the symmetry group is C_{4v} . Thus, the scattering amplitude $\delta f(\vec{k}^{(F)}, \vec{k}^{(I)}; \{\vec{R}\})$ consists of a sum of the two amplitudes $\delta f_{A\alpha}^{(1)}(\vec{Q}_{\parallel})$, $\delta f_{B\alpha}^{(1)}(\vec{Q}_{\parallel})$, each weighted by an eigenvector amplitude. If we consider, say, scattering by the two normal modes normal to the surface, then as we saw in Ref. 3 the amplitudes $u_1^{(A)}$ and $u_1^{(B)}$ are fully determined once the ratio of the two frequencies $\omega_1^{(+)}$ (the CO stretch) and $\omega_1^{(-)}$ (the C-Ni mode) are known. A similar statement applies to modes polarized parallel to the surface.

Our calculations show that the energy variation of the EELS cross section is rather insensitive to the value chosen for the ratio $\omega_1^{(+)}/\omega_1^{(-)}$. We illustrate this in Fig. 1, where for a particular scattering geometry we plot $dP_{\omega_1^{(+)}}^{(+)} / d\Omega$, the probability per unit solid angle, of exciting the $\omega_1^{(+)}$ mode. We have fixed the value of the frequency of the $\omega_1^{(-)}$ mode (the C-Ni mode) at the value 480 cm^{-1} measured by Andersson,⁹ and three values of $\omega_1^{(+)}$ have been used to generate the ratio of the vibrational amplitudes of the two nuclei. The solid curve is calculated for the measured value of the CO stretch frequency, $\omega_1^{(+)} = 2070 \text{ cm}^{-1}$, the dashed curve is calculated for the choice $\omega_1^{(+)} = 2890 \text{ cm}^{-1}$, and the dot-dashed curve for 1655 cm^{-1} . We see that the variation of $\omega_1^{(+)}$ over a rather wide range

leaves the energy variation of $dP_{\omega_1^{(+)}}/d\Omega$ unaffected, but does somewhat alter the overall magnitude of the cross section. The latter effect is as expected, since the EELS cross section increases as the zero-point amplitude of the mode responsible for the scattering increases (we have $\hbar\omega_1^{(+)} \ll k_B T$ here), and lowering $\omega_1^{(+)}$ increases the zero-point amplitude.

We have found very similar results in our calculations of the EELS cross section for scattering from the $\omega_1^{(-)}$ mode. These results show that we do not require full knowledge of the factors that control the eigenvectors to perform reliable calculations of $(dP/d\Omega)$. We may understand this as follows. For the CO molecule in the gas phase, the center of mass of the molecule remains fixed when the CO stretch vibration is excited. This leads to the amplitude ratio $(u_1^{(A)}/u_1^{(B)}) = -(M_B/M_A)$. When the CO is adsorbed onto the substrate and the stretching vibration is excited, the center of mass of the molecule wobbles, but the correction to the gas-phase ratio for (u_1^A/u_1^B) is of order $(\omega_1^{(-)}/\omega_1^{(+)})^2$, and this is very small. One may see this from the formulas in Appendix A of Ref. 3. Thus, the fact that $\omega_1^{(-)} \ll \omega_1^{(+)}$ means that for the CO stretch vibration, the ratio $(u_1^{(A)}/u_1^{(B)})$, and consequently the energy variation of the EELS cross section, is not greatly affected by the existence of the C-Ni bond. Also, the amplitude of the center-of-mass wobble is small in the limit $\omega_1^{(-)} \ll \omega_1^{(+)}$. Similarly, when we consider scattering from the $\omega_1^{(-)}$ mode, we have $u_1^{(A)} \approx u_1^{(B)}$ in the

limit $\omega_1^{(-)} \ll \omega_1^{(+)}$, since the "stiff spring" between the carbon and oxygen nuclei does not allow relative motion of these two constituents.

We expect results similar to these will hold for a wide variety of adsorbed layers formed from molecules, where modes similar in character to gas-phase normal modes have frequencies high compared to modes that are rotations or translations of the gas-phase species hindered by bonding to the substrate. The eigenvectors of the gas-phase motion may be used in these instances, with no great cost in quantitative accuracy.

We remark that all the calculations in Fig. 1, and those reported in the remainder of the paper, consider geometries where the incident electron wave vector $\vec{k}^{(I)}$, the scattered electron wave vector $\vec{k}^{(F)}$, and the normal to the surface \hat{n} , lie in the same plane. We call this the scattering plane. Furthermore, in all the calculations the scattering plane is oriented parallel to a [100] direction in the surface.

For most scattering geometries for the CO layer adsorbed on Ni(100), we find the position and shape of the structures in the EELS cross section are quite sensitive to the carbon-oxygen bond length, and at the same time are relatively insensitive to the carbon-nickel bond length. The reason for this is that the electron-phonon matrix element is small for forward scattering from the carbon and oxygen layer, and is much larger for backscattering from it. Thus, most of the electrons which emerge from the surface have been backscattered from the carbon and oxygen layer without penetrating through to the substrate. We next present a series of calculations which illustrate these points.

In Fig. 2, for two values of the CO bond length,

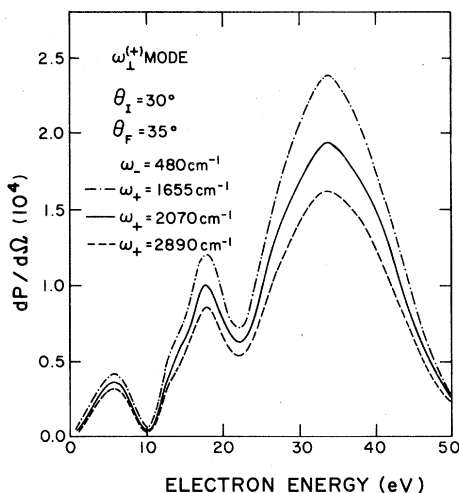


FIG. 1. The probability per unit solid angle ($dP/d\Omega$) for exciting the CO stretch mode ($\omega_1^{(+)}$), as a function of electron energy for a particular scattering geometry. The incident electron wave vector, outgoing electron wave vector, and normal to the surface all lie in the same plane, the scattering plane. The scattering plane is aligned along a [100] direction.

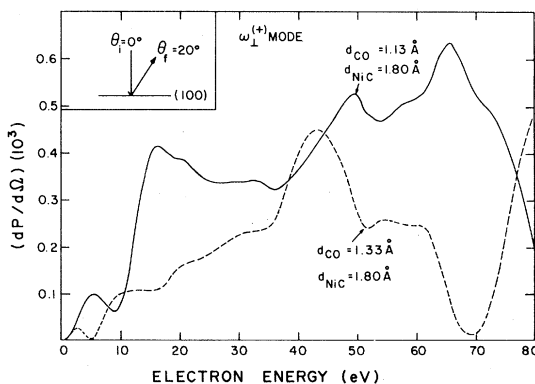


FIG. 2. The energy variation of the probability per unit solid angle for scattering from the $\omega_1^{(+)}$ mode for the scattering geometry shown in the inset. For both curves, the Ni-C distance has been chosen equal to 1.80 Å, and the CO bond length has been varied.

we show the energy variation of the probability ($dP^{(+)} / d\Omega$) per unit solid angle for scattering by the $\omega_1^{(+)}$ mode. In both calculations, the C-Ni perpendicular distance has been fixed at 1.80 Å, while two values of the CO bond length which differ by 0.2 Å have been employed. We see striking differences between the two curves. The broad peak in the curve for $d_{CO} = 1.13$ Å is missing from the curve calculated for $d_{CO} = 1.33$ Å, and an interference minimum occurs near 70 eV incident energy in the 1.33 Å curve, while a well-defined peak appears near this energy for the curve calculated for $d_{CO} = 1.13$ Å.

In contrast to the sensitivity to the CO bond length displayed in Fig. 2, we find the EELS cross sections are remarkably insensitive to the spacing between the CO layer and the Ni substrate. This we illustrate in Fig. 3, where we show calculations of ($dP^{(+)} / d\Omega$) for scattering from the $\omega_1^{(+)}$ mode for $d_{CO} = 1.13$ Å and for two values of the Ni-C spacing. There are distinct differences between the two curves, but these are rather subtle. While we have found scattering geometries which produce energy variations for ($dP / d\Omega$) sensitive to the C-Ni spacing, as we shall see shortly, on the whole the results are not very sensitive to this parameter.

The reason is that the amplitude for backscattering from the CO layer, with emission of a vibrational quanta, is in general appreciably larger than the corresponding amplitude in the forward direction. Furthermore, the structure in ($dP / d\Omega$) has its primary origin in interference between the term proportional to $\delta f_{A\alpha}^{(-)}(\vec{Q}_{\parallel})$, and that proportional to $\delta f_{B\alpha}^{(1)}(\vec{Q}_{\parallel})$; both $|\delta f_{A\alpha}^{(-)}(\vec{Q}_{\parallel})|^2$ and $|\delta f_{B\alpha}^{(1)}(\vec{Q}_{\parallel})|^2$ are smooth functions of energy. Thus, ($dP / d\Omega$) is sensitive to the CO bond length, but is not affected greatly by variations in the C-Ni bond length.

We may illustrate this point as follows. Suppose we consider a layer of CO molecules embedded in

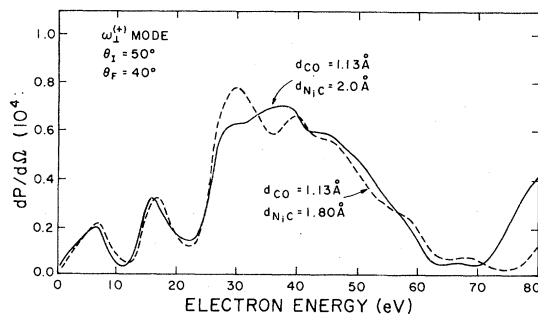


FIG. 3. The energy variation of $dP/d\Omega$, the probability per unit angle for scattering from the $\omega_1^{(+)}$ mode, for two values of the C-Ni spacing and for the C-O bond length indicated. The scattering plane has been aligned with the [100] direction.

the (complex) inner potential used in the above calculation, and we define for either the oxygen or the carbon layer two scattering amplitudes Q_{00}^{++} and Q_{00}^{+-} as follows. For the carbon layer, for example, the quantity Q_{00}^{+-} is the amplitude that the electron approaches the carbon layer with angle of incidence θ_I (from below; the half space $z < 0$ is the vacuum) and is *backscattered* from the layer to emerge with angle θ_F relative to the surface normal, after excitation of a vibrational quanta. We include in the calculation of Q_{00}^{+-} all multiple-scattering events within the carbon layer as the site of vibrational excitation is approached, and as the electron exits the layer; i.e., Q_{00}^{+-} is the amplitude for backscattering with vibrational excitation from an isolated carbon layer. Similarly, Q_{00}^{++} is the amplitude for *forward* scattering through the layer with vibrational excitation, again to emerge with angle θ_F relative to the normal. The formulas for both Q_{00}^{+-} and Q_{00}^{++} are given as Eq. (3.18) of Ref. 3. For a plane of atoms with up-down reflection symmetry, $Q_{00}^{++} = Q_{00}^{--}$, and $Q_{00}^{+-} = Q_{00}^{-+}$. The magnitude and angle variation of the amplitudes for forward scattering through or backscattering from the oxygen layer have similar behaviors as those of scattering from the carbon layer, so many qualitative aspects of scattering from the CO layer may be appreciated by studying the scattering from the individual layer.

In Fig. 4, for $\theta_I = 50^\circ$ and selected energies, and for scattering from the $\omega_1^{(+)}$ mode, we show both $|Q_{00}^{+-}|$ and $|Q_{00}^{++}|$ for the carbon layer as a function of θ_F . For almost all of the angles explored (but not everywhere) we have $|Q_{00}^{+-}| \gg |Q_{00}^{++}|$, so the majority of the electrons are backscattered from the carbon layer and never get through to the substrate. Note that the ordinate of Fig. 4 is a log-

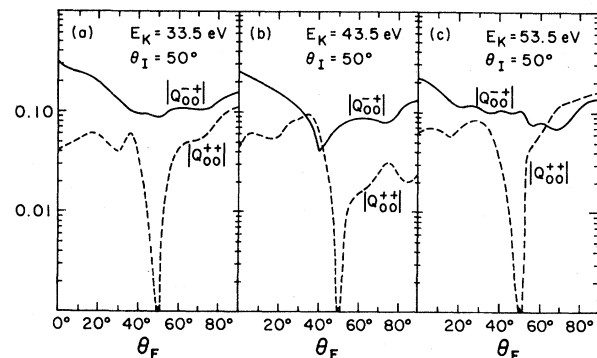


Fig. 4. For an angle of incidence $\theta_I = 50^\circ$, we plot the quantities $|Q_{00}^{+-}|$, $|Q_{00}^{++}|$ defined in the text as a function of the angle θ_F between the scattered electron wave vector and the normal to the carbon layer for (a) an incident electron energy of 33.5 eV, (b) an incident energy of 43.5 eV, and (c) an incident energy of 53.5 eV. The calculations assume the electrons excite the $\omega_1^{(+)}$ mode.

arithmetic scale. The zero in $|Q_{00}^{++}|$ at $\theta_F = \theta_I = 50^\circ$ is an illustration of a selection rule, and this will be discussed in Sec. III.

We may use plots that compare $|Q_{00}^{+-}|$ with $|Q_{00}^{++}|$ for carbon and oxygen to search for regimes of angle and energy where $(dP/d\Omega)$ exhibits sensitivity either to the CO or the C-Ni spacing. One example is illustrated in Fig. 5, where for a mode with displacements parallel to the surface, we show similar plots of $|Q_{00}^{+-}|$ and $|Q_{00}^{++}|$ for the carbon layer. The mode considered has displacements *parallel* to the scattering plane, which as in the other calculations is aligned along the [100] direction. We call the two normal modes of this polarization $\omega_x^{(+)}$ and $\omega_x^{(-)}$, and the calculations shown are for the high-frequency $\omega_x^{(+)}$ mode. We have calculated the eigenvector of the mode using the frequencies $\omega_x^{(+)} = 460 \text{ cm}^{-1}$ and $\omega_x^{(-)} = 65 \text{ cm}^{-1}$ taken from Ni carbonyl compounds.

From Fig. 5, we see that for exit angles in the range $\theta_F \cong 20^\circ$, we have $|Q_{00}^{++}| \gg |Q_{00}^{+-}|$. Now most of the electrons that strike the adsorbed carbon layer are scattered in the *forward* direction after vibrational excitation, and must be backscattered from the substrate before they can emerge into the vacuum. With this scattering geometry, $(dP/d\Omega)$ should exhibit features sensitive to the C-Ni spacing.

We illustrate this in Fig. 6, where for $\theta_I = 50^\circ$ and $\theta_F = 20^\circ$, we calculate the energy variation of $(dP/d\Omega)$ for excitation of the $\omega_x^{(+)}$ mode. This is done for $d_{CO} = 1.13 \text{ \AA}$, and several values of the Ni-C separation. We now see considerable sensitivity to the Ni-C spacing as we expect from Fig. 5. As d_{Ni-C} is shortened from 2.0 to 1.6 \AA , the trend is for the structures in $(dP/d\Omega)$ to shift to higher energies, with shifts as large as 10 eV evident in the figure. When these results are compared to those in Fig. 3, we see that study of the

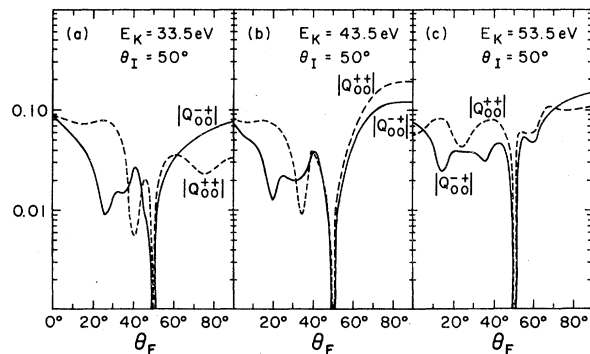


FIG. 5. The quantities $|Q_{00}^{+-}|$ and $|Q_{00}^{++}|$ for the carbon layer calculated for $\theta_I = 50^\circ$ as a function of θ_F for the $\omega_x^{(+)}$ mode. The incident electron energy has been chosen to be (a) 33.5 eV, (b) 43.5 eV, and (c) 53.5 eV.

behavior of $|Q_{00}^{+-}|$ and $|Q_{00}^{++}|$ for carbon and oxygen is a useful way of locating regimes of energy and angle where the behavior of $(dP/d\Omega)$ is sensitive to distances between the adsorbate layers or between the adsorbate and the substrate. It must be kept in mind that the x - and y -polarized modes are degenerate for our CO molecular on its site of C_{4v} symmetry. But as we shall see in Sec. III, when both $\vec{k}^{(I)}$ and $\vec{k}^{(F)}$ lie in a reflection plane, the cross section for scattering from the y -polarized mode vanishes.

The zero at $\theta_I = \theta_F$ in $|Q_{00}^{++}|$ in Fig. 4, along with those in both $|Q_{00}^{+-}|$ and $|Q_{00}^{++}|$ in Fig. 5 are not accidental, but are in fact symmetry determined. There are a series of symmetry-induced zeros in the EELS cross sections in the impact-scattering mechanism. Some of these were discussed by us earlier,⁴ and we now turn to a more detailed analysis of these features, which should prove most useful to the experimentalist.

III. SELECTION RULES IN IMPACT SCATTERING

In Ref. 4 we presented a brief discussion of selection rules that operate in the impact-scattering regime. We now turn to a more complete discussion of these rules. These rules are partially illustrated by the results presented in Ref. 4, and the results displayed in Sec. II of the present paper.

The geometry considered in this discussion is illustrated in Fig. 7. As in Sec. II, we consider a scattering configuration in which the wave vector $\vec{k}^{(I)}$ of the incident electron, the $\vec{k}^{(F)}$ of the scattered electron, and the normal \hat{n} to the surface, all lie in the same plane which is here the xz plane. As above, we call the xz plane the

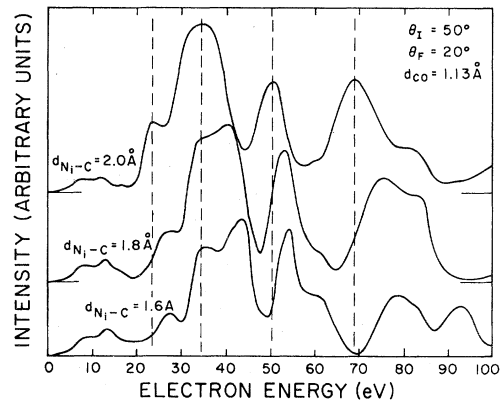


FIG. 6. For $d_{CO} = 1.13 \text{ \AA}$ and several values of d_{Ni-C} , we calculate the energy variation of $dP/d\Omega$ for exciting the $\omega_x^{(+)}$ mode. The incident angle $\theta_I = 50^\circ$ and $\theta_F = 20^\circ$, where Fig. 5 suggests $(dP/d\Omega)$ should be sensitive to the C-Ni spacing.

scattering plane.

We also confine our attention to an adsorbate atom or a linear diatomic molecule such as CO in an adsorption site with symmetry sufficiently high that the normal modes of vibration are polarized purely normal to the surface, or purely parallel to it. We wish the eigenvectors to transform under rotations, reflections, etc., as vector quantities. For more complex molecules, or possibly for a diatomic molecule which "lies down" on the surface, the eigenvectors may have very different transformation properties, and the selection rules outlined here will fail to apply. We touch on these more general cases only briefly at the end of the present section. Also, throughout this section our attention is confined to one-phonon loss events.

Note that for our case the eigenvectors which describe vibrations parallel to the surface may be separated into sets which describe motions parallel to two mutually orthogonal directions. We consider the selection rules which operate in three cases.

A. Vibrational modes polarized parallel to the surface and normal to the scattering plane (y -polarized modes)

Consider scattering produced by a vibrational mode polarized along the \hat{y} direction in Fig. 7(a). The scattering amplitude must vanish in the following circumstances.

(i) Suppose that the nature of the adsorption site is such that the operation of reflection R_{xz} (through the xz plane) is a good symmetry opera-

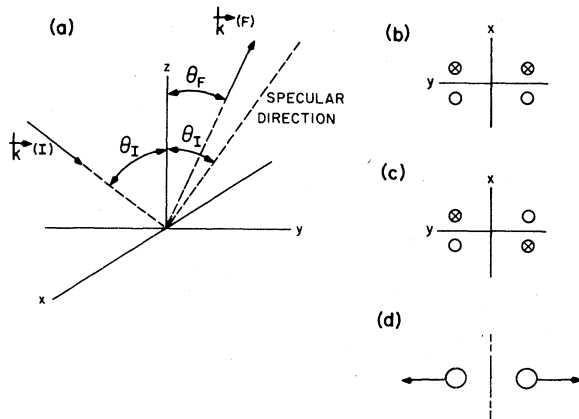


FIG. 7. (a) The scattering geometry which forms the basis for the discussion of the impact scattering selection rules. Both $\vec{k}^{(I)}$ and $\vec{k}^{(F)}$ lie in the xz plane. (b) Example of a geometry for which the xz plane is a reflection plane (z normal to xy plane). (c) Example of a geometry where the z axis is a twofold axis, but the xz plane is not a reflection plane. (d) An example of a diatomic molecule which "lies down" on the surface and for which the parity of the stretching vibration is even.

tion. Then the EELS cross section must vanish for *all* wave vectors $\vec{k}^{(F)}$ in the xz plane. The reason is that the wave function $|\psi_I\rangle$ of the electron in the initial state, and that $|\psi_F\rangle$ of the electron in the final state are both *even* under R_{xz} . This is true, of course, not simply for the incoming and outgoing plane waves in the vacuum outside the crystal, but for the entire electron wave function, including the portion in the crystal. In effect, the calculation of the EELS cross section involves evaluation of a matrix element that "sandwiches" the change in potential δV produced by the ionic motion, between $|\psi_I\rangle$ and $|\psi_F\rangle$. Since δV is necessarily odd under R_{xz} , the EELS scattering amplitude and the single-layer amplitudes $Q_{00}^{(\pm)}$ vanish whenever $\vec{k}^{(F)}$ lies in the xz plane.

(ii) Suppose the nature of the adsorption site is such that there is twofold rotational symmetry about the z axis. This is clearly a situation different than that just considered. As an illustration, we show in Fig. 7(b) a geometry for which R_{xz} is a good symmetry operation, but the z axis is not a twofold axis. In Fig. 7(c) a geometry is illustrated for which the z axis is a twofold axis, but R_{xz} is not a good symmetry operation.

In this situation, the EELS scattering amplitude and Q_{00}^{+-} , Q_{00}^{+} vanish only for $\vec{k}^{(F)}$ directed along the specular direction. That this is so may be seen as follows. Let $\vec{k}^{(F)}$ lie along the specular direction. Then a twofold rotation about the \hat{z} axis changes the sign of the eigenvector \vec{u} associated with the vibrational mode, and hence changes the sign of δV . Also, we have $\vec{k}^{(I)} \rightarrow -\vec{k}^{(F)}$, and $\vec{k}^{(F)} \rightarrow -\vec{k}^{(I)}$ under this operation. If we assume also that time reversal is a good symmetry operation and the scattering is quasi-elastic so we ignore the difference between the magnitude of $\vec{k}^{(I)}$ and $\vec{k}^{(F)}$ in calculating the electron wave function, the combination of the twofold rotation and time reversal leaves the electron scattering geometry invariant, but changes the sign of δV . This is sufficient to ensure that for specular $\vec{k}^{(F)}$, the total scattering amplitude, Q_{00}^{++} and Q_{00}^{--} vanish.

The single-layer amplitudes Q_{00}^{++} and Q_{00}^{--} will vanish for $\vec{k}^{(F)}$ in the forward direction if the midplane of the layer is a reflection plane, the z axis is a twofold axis and we need time-reversal symmetry.

B. Vibrational modes polarized parallel to the surface and parallel to the scattering plane (x -polarized modes)

We consider modes polarized parallel to the surface, and parallel to the scattering plane in Fig. 7(a). For the EELS cross section and single-layer amplitudes Q_{00}^{-+} and Q_{00}^{-} , and Q_{00}^{+-} , we again

have two selection rules. These are the following.

(i) Suppose reflection in the yz plane is a good symmetry operation. Then within the approximation that we may take wave vector $\vec{k}^{(F)}$ of the scattered electron equal in magnitude to that $\vec{k}^{(I)}$ of the incident electron, the combined effects of R_{yz} and time-reversal symmetry require the EELS cross section and Q_{00}^{+-} , Q_{00}^{-+} for scattering from the x -polarized mode to vanish when $\vec{k}^{(F)}$ is directed along the specular direction.

We see an illustration of this selection rule in Fig. 5 of the present paper. Note that for each energy for which calculations of $|Q_{00}^{+-}|$ are displayed, this quantity vanishes identically when the electron emerges along the specular direction. This zero is a consequence of the selection rule just described. We also show in Fig. 8 calculations of the angular variation of $(dP/d\Omega)$ for the two x -polarized modes of the adsorbed CO. In each case, the EELS cross section $(dP/d\Omega)$ vanishes along the specular direction. Finally, in our earlier note this selection rule was discussed,² and calculations were presented which

illustrate it.

(ii) Suppose the scattering plane is arranged so that a rotation of 180° about the z direction is a good symmetry operation. Then this rotation symmetry, combined with time-reversal symmetry along with the assumption $|\vec{k}^{(I)}| \cong |\vec{k}^{(F)}|$ requires the EELS cross section Q_{00}^{-+} and Q_{00}^{+-} to vanish along the specular direction.

For layer amplitudes Q_{00}^{+-} and Q_{00}^{-+} to vanish in the forward direction, we need the y axis to be a twofold rotation axis, and we also need time-reversal symmetry. These quantities vanish also if the z axis is a twofold axis, and there is in addition reflection symmetry in the xy plane combined with time-reversal symmetry.

C. Vibrational modes polarized perpendicular to the surface (z -polarized modes)

There is a selection rule that applies here to more limited usefulness than those just described. Consider a plane of adsorbed atoms (or perhaps a plane of substrate atoms). Let Q_{00}^{+-} , Q_{00}^{++} be the amplitudes for backscattering from the plane and for scattering through the plane. Then for the geometry illustrated in Fig. 7(a), if the plane has twofold rotational symmetry about the y axis, this symmetry combined with time-reversal symmetry and the assumption $|\vec{k}^{(I)}| = |\vec{k}^{(F)}|$ requires Q_{00}^{++} to vanish in the forward direction, when $\theta_F = \theta_I$. This selection rule is illustrated in Fig. 4, where for each energy considered, we see that $|Q_{00}^{++}|$ vanishes when $\theta_F = \theta_I$. Also Q_{00}^{++} must vanish in the forward direction if the z axis is a twofold axis and if the xy plane is a reflection plane. Then a twofold rotation about z , combined with reflection in the xy plane and time reversal requires Q_{00}^{++} to vanish in the forward direction. However, for z -polarized mode, even for $\theta_I = \theta_F$ and Q_{00}^{-+} do not vanish.

In circumstances where backscattering from the substrate makes a substantial contribution to the cross section, this selection rule can cause a dip in the impact-scattering cross section for scattering from z -polarized modes. While this dip may be partially or totally obscured by the dipole scattering allowed for these same modes, it may be observable for modes with large impact-scattering cross sections or small values of the dynamic effective charge (polarizability derivative). Unfortunately, for the case of the $c(2 \times 2)$ overlayer of CO on Ni(100) examined here, we saw in Sec. II that $|Q_{00}^{-+}| \gg |Q_{00}^{++}|$ for the z -polarized modes. No dip shows up in the total cross section, to graphical accuracy. In Fig. 9, we show calculations of the angular distribution of electrons scattered by the z -polarized modes, and we see a smooth angular variation, with no

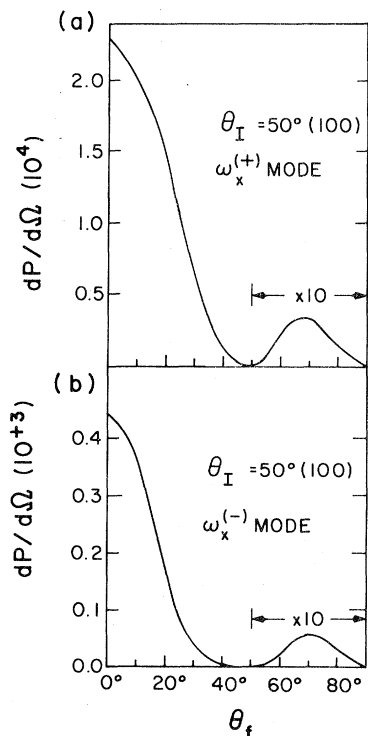


FIG. 8. Calculations of $(dP/d\Omega)$ for the x -polarized modes (vibrations parallel to the surface and parallel to the scattering plane), for the case where the scattering plane is aligned parallel to the [100] direction, and the selection rule requires $(dP/d\Omega)$ to vanish along the specular direction. The angle of incidence is 50° , and the calculations are carried out for an incident electron energy of 6.5 eV.

sign of a dip at $\theta_F = \theta_I = 50^\circ$. In Fig. 9, so the reader may appreciate the relative sizes of various contributions to the cross section, we have decomposed the total cross section into that part which comes from the oxygen layer alone, that from the carbon layer, and the interference term between the two. This completes our discussion of the selection rules that operate in the impact-scattering regime. We conclude with a few general comments.

We have invoked one assumption that goes beyond symmetry considerations to demonstrate some of the rules above, and this is that the energy change of the electron is sufficiently small that we may suppose that $|\vec{k}^{(F)}| \cong |\vec{k}^{(I)}|$. The selection rules that depend on this assumption may well break down for experiments carried out in energy regimes where the reflectivity varies rapidly with electron energy, so at the outgoing

electron energy, the wave function is substantially different than that at the incident energy. This can happen, for example, in the near vicinity of the fine-structure resonances observed often at low impact energies.¹⁰ If one wishes to exploit these selection rules, care should be taken to carry out experiments in energy regimes where the reflectivity varies little over the relevant range of energy and angle. We currently have underway a new series of calculations which include the effect of the image potential, so the influence of the fine-structure resonances will be included fully. Their influence on the selection rules just described, and comparison with experimental data, will be discussed in a subsequent publication.

We have also invoked time-reversal symmetry and used it in combination with reflection or rotational symmetry to establish most of the rules. It is interesting to explore the selection rules for EELS experiments carried out on ferromagnetic surfaces, where time-reversal symmetry breaks down. A lengthy discussion of the selection rules is required here, and we shall present such an analysis elsewhere. Note that for electrons incident on the ferromagnetic metals, the incoming electron feels the presence of the magnetism not only from spin-orbit coupling, which is relatively small in the ferromagnetic transition metals, but from the strong Coulomb interactions in combination with the Pauli principle. This point has been emphasized by Feder in his analysis of spin-dependent elastic scattering of electrons from the surfaces of ferromagnetic metals.¹¹ Thus, there are very substantial differences in the wave function of an electron incident with spin parallel to the magnetization of the substrate, or antiparallel to it.

It is important to note that the selection rules also require the normal coordinate of the mode responsible for the scattering transform under reflections and rotations like a vector quantity. It is easy to find an example of a mode that fails to satisfy this requirement. Consider the stretching vibrations of a diatomic molecule which lies parallel to the surface. If we consider a homopolar molecule, then as illustrated in Fig. 7(d), under reflection through the dotted plane, the stretch vibration has even parity rather than odd parity as in the examples for which the selection rule holds. When more complex molecules, such as NH_3 or C_2H_2 are considered as adsorbates, these will be a subset of modes for which they do not operate; the rules may then assist the experimentalist in making symmetry assignments to the various modes detected in an EELS experiment.

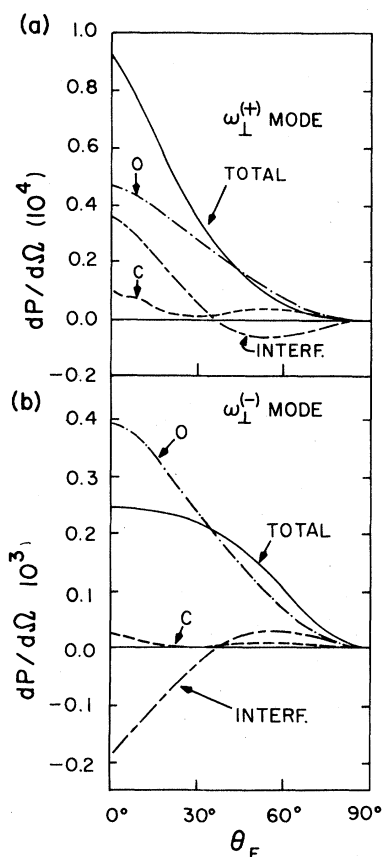


FIG. 9. The angular distribution of electrons scattered by the two normal modes polarized perpendicular to the surface, the $\omega_{\perp}^{(+)}$ mode (CO stretch), and the $\omega_{\perp}^{(-)}$ mode (C-Ni mode). The angle of incidence is 50° and the incident electron energy is 6.5 eV. We have decomposed the cross section in a piece that comes from scattering off the layer of oxygen nuclei alone, from the C layer alone, and the interference term between the two.

ACKNOWLEDGMENTS

This work has been supported by the Department of Energy through Grant Nos. DE-AC02-79ER10431

and DOE AT03-79-ER10432. We wish to thank Professor Harald Ibach for a number of helpful comments.

¹For a review of the early generation of experiments and the related theory, see H. Froitzheim, in *Electron Spectroscopy for Surface Analysis*, Topics in Current Physics, edited by H. Ibach (Springer, New York, 1976), Vol. 4, and see also D. L. Mills, *Prog. Surf. Sci.* 8, 143 (1977). A discussion of more recent experiments, with references, can be found in the paper by R. F. Willis, W. Ho, and E. W. Plummer, *Surf. Sci.* 80, 593 (1979).

²H. Ibach and D. Bruchman, *Phys. Rev. Lett.* 41, 958 (1978).

³C. H. Li, S. Y. Tong, and D. L. Mills, *Phys. Rev. B* 21, 3057 (1980).

⁴S. Y. Tong, C. H. Li, and D. L. Mills, *Phys. Rev. Lett.* 44, 407 (1980).

⁵E. Evans and D. L. Mills, *Phys. Rev. B* 5, 4126 (1972); 7, 853 (1973).

⁶For a discussion of the conditions that must be met for this rule to be valid, see D. L. Mills, *Surf. Sci.* 48, 59 (1975).

⁷H. Ibach, *Surf. Sci.* 66, 56 (1977).

⁸J. W. Davenport, W. Ho, and J. R. Schrieffer, *Phys. Rev. B* 17, 3115 (1978).

⁹S. Andersson, *Solid State Commun.* 21, 75 (1977).

¹⁰E. G. McRae, *Rev. Mod. Phys.* 51, 541 (1979).

¹¹R. Feder, *Surf. Sci.* 63, 283 (1977).